NBSIR 84-2809

Development of Power System Measurements -- Quarterly Report April 1, 1983 to June 30, 1983

U.S. DEPARTMENT OF COMMERCE
National Bureau of Standards
Center for Electronics and Electrical Engineering
Electrosystems Division
Washington, DC 20234

February 1984

Prepared for:
Department of Energy
Division of Electric Energy Systems
00 Independence Avenue, SW
ashington, DC 20585

NBSIR 84-2809

DEVELOPMENT OF POWER SYSTEM MEASUREMENTS -- QUARTERLY REPORT APRIL 1, 1983 TO JUNE 30, 1983

R. E. Hebner, Editor

U.S. DEPARTMENT OF COMMERCE
National Bureau of Standards
Center for Electronics and Electrical Engineering
Electrosystems Division
Washington, DC 20234

February 1984

Prepared for:
Department of Energy
Division of Electric Energy Systems
1000 Independence Avenue, SW
Washington, DC 20585

U.S. DEPARTMENT OF COMMERCE, Malcolm Baldrige, *Secretary*
NATIONAL BUREAU OF STANDARDS, Ernest Ambler, *Director*

Foreword

This report summarizes the progress on four technical investigations during the third quarter of FY 83. Although reasonable efforts have been made to ensure the reliability of the data presented, it must be emphasized that this is an interim report so that further experimentation and analysis may be performed before the conclusions from any of these investigations are formally published. It is therefore possible that some of the observations presented in this report will be modified, expanded, or clarified by our subsequent research.

TABLE OF CONTENTS

LIST OF FIGURES

LIST OF FIGURES (cont.)

LIST OF TABLES

DEVELOPMENT OF POWER SYSTEM MEASUREMENTS -- QUARTERLY REPORT
April 1, 1983 to June 30, 1983

R. E. Hebner, Editor

This report documents the progress on five technical investigations sponsored by the Department of Energy. Three were performed by the Electrosystems Division, the National Bureau of Standards, the fourth by the Department of Electrical Engineering of the University of Southern California, and the fifth by the College of Engineering at the University of South Carolina. The work described covers the period from April 1, 1983 to June 30, 1983. The report emphasizes the calibration of instruments designed to measure the 60-Hz electric field in biological exposure facilities, the effect of water on SF_6 corona discharges, the measurement of failure mechanisms in liquid/solid and gas/solid insulating systems, and the development and behavior of active insulators.

Key words: composite insulation; electric fields; high voltage; insulation; liquid breakdown; SF_6; space charge; transformer oil.

1. INTRODUCTION

Under an interagency agreement between the U.S. Department of Energy (DOE) and the National Bureau of Standards (NBS), the Electrosystems Division, NBS, has been providing technical support for DOE's research on electric energy systems. This support is concentrated in three areas -- the measurement of electric fields, the measurement of partial discharge phenomena in gaseous dielectrics, and the measurement of interfacial electrostatic field distributions and of space charge density. The technical progress made during the quarter April 1, 1983 to June 30, 1983 is summarized in this report. Some of this work is being performed at the University of Southern California and the University of South Carolina under grants from NBS.

2. ELECTRIC FIELD MEASUREMENTS
Subtask Nos. 01 and 02

The objectives of this investigation are to develop methods to evaluate and calibrate instruments which are used, or are being developed, to measure the electric field, air conductivity, the space charge density, and ion current density in the vicinity of high-voltage dc transmission lines and in apparatus designed to simulate the transmission line environment; to provide electrical measurement support for DOE-funded efforts to determine the effects of ac fields on biological systems, and to provide similar support for biological studies which will be funded by the State of New York.

During the current reporting period the performance of free-body dipole electric fieldmeters, which had been calibrated for use in nearly uniform power frequency electric fields, was examined under nonuniform field conditions. Measurements of nonuniform electric fields produced with a sphere-plane electrode system were found to support the theory that free-body probes calibrated in a uniform field could be used to measure significantly nonuniform

fields with small error. Figure 1 shows that measurements of a nonuniform electric field obtained with commercial field probes with rectangular geometries, (b) and (c), agree with those obtained with a miniature spherical probe (a) developed at NBS within experimental uncertainty (less than ±3% for all measurements).

Free-body probes such as those tested have been used for measuring the electric field strength near ground level in the vicinity of transmission lines where the field changes slowly as a function of position, as well as in substations and homes where fields are less uniform. The theory and test results have recently been submitted to the Institute for Electronics and Electrical Engineering (IEEE) Transactions on Electrical Insulation for publication.

NBS staff members visited the University of Texas Health Science Center in San Antonio, Texas and the University of Wisconsin-Parkside to perform measurements of 60-Hz magnetic fields and observe procedures employed by researchers for the measurement of several related electrical quantities. The investigators at both universities are performing in vitro biological studies of cells exposed to 60-Hz electric and magnetic fields. The studies are funded by the Department of Health of the State of New York.

The second revision of an International Electrotechnical Commission (IEC) draft standard for the measurement of power frequency electric fields was completed at NBS and distributed to members of Working Group 6 of TC42 for further comments. Copies of the draft were also distributed to members of the IEEE HVTT Subcommittee and IEEE PES Working Group on AC Fields, to obtain additional comments from the U.S technical community.

During the next quarter a draft of a primer for measurement of several electrical parameters which must be controlled during biological studies with 60-Hz electric and magnetic fields will be written. At least one visit will be made to a laboratory where 60-Hz biological studies are being performed with support from New York State. Comments on the latest revision of the IEC draft standard for measurement of 60-Hz electric fields will be received during the next quarter from members of IEC TC42 Working Group 6. If a consensus is near on the contents of the draft standard, a meeting of the working group will be planned to prepare a final draft. If time permits, some tests associated with the performance of ion counters operating in the ground plane will be made in the NBS parallel plate structure. These measurements were originally planned for the current reporting period.

For further information contact Dr. M. Misakian, (301) 921-3121, National Bureau of Standards, Washington, DC.

3. TECHNICAL ASSISTANCE FOR FUTURE INSULATION SYSTEMS RESEARCH
Subtask No. 03

The objectives of this project are the development of diagnostic techniques to monitor, identify, and predict degradation in future compressed gas, electrical insulating systems under normal operating conditions. The focus is on the fundamental information and data needed to improve test design and performance evaluation criteria. The investigation of partial discharges (corona) in gaseous dielectrics is emphasized. This phenomenon gives rise to degradation of the gas under high electrical stress which leads to breakdown.

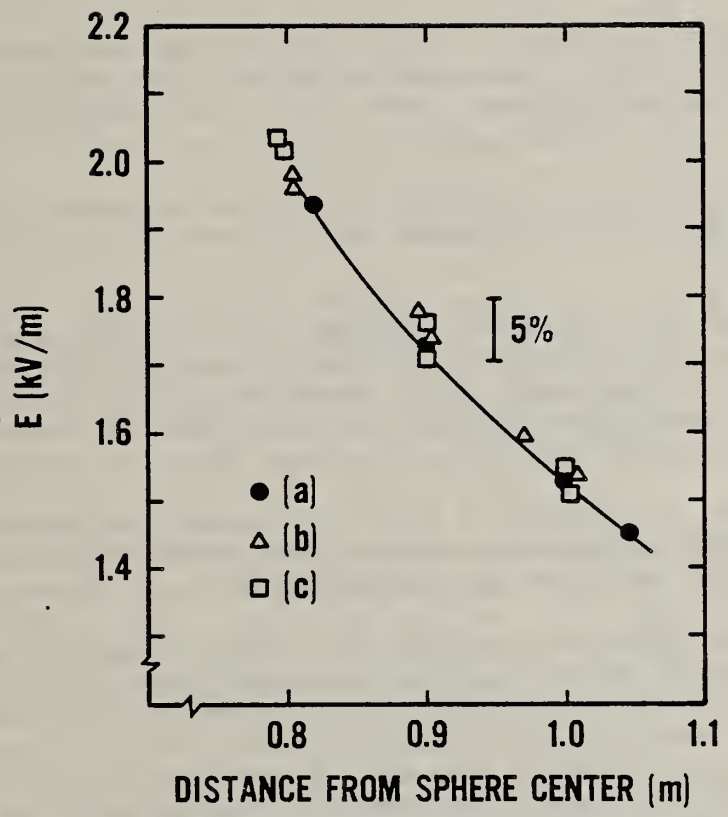

Figure 1. Measurement of nonuniform electric field with miniature NBS spherical probe (a) and large commercial probes with rectangular geometries (b) and (c).

Measurement of partial discharge inception in highly nonuniform fields may prove to be a preferred method to determine dielectric strength of electronegative gases.

The planned activities for FY83 include:

1) Preparation of conference and archival papers on the effect of radiation in enhancing electric discharge initiation near a positively stressed electrode in compressed SF_6 and O_2;

2) Extension of our previous measurements [1] of the production rates of oxyfluorides in SF_6 corona discharges to include negative discharges as well as other gas pressures and discharge power levels, and preparation of the results for publication in an archival paper;

3) Identification of the predominant gaseous decomposition products from corona in one or more of the following gas mixtures: $SF_6 + N_2$, $SF_6 + CO_2$, and $SF_6 + c\text{-}C_4F_8 + CHF_3$;

4) Evaluation of a thin-film, aluminum oxide hygrometer probe for calibration of a gas chromatograph-mass spectrometer (GC/MS) used to measure trace quantities of water vapor in SF_6 and other gaseous dielectrics, and extension of our previous measurements on the effects of trace levels of H_2O on electron avalanche growth and corona discharge characteristics in SF_6; and

5) Design and construction of a drift tube-mass spectrometer system to evaluate proposed measurements to identify and characterize corona-generated ion species in air, SF_6, and other gas dielectrics.

Activity 1 has been completed and during the past quarter an archival paper describing the results of this work has been published [2]. Also during this quarter, the results of our previous survey and critical evaluation of electron transport data in electronegative gases were published in an archival paper [3]. Additional measurements and analyses of data were carried out as part of activities 2 and 4. The results obtained in activity 2 will be highlighted in this report. For activity 4 preliminary results were obtained on the correlation between the responses of thin-film, aluminum oxide hygrometer probes and the gas chromatograph-mass spectrometer (GC/MS) for detection of trace levels of water vapor in static SF_6 gas. Recent measurements in our laboratory indicate that the GC/MS is much more sensitive than the hygrometer probe for detection of H_2O at concentrations below about 10 ppm_v (parts per million by volume). At low H_2O concentrations (<50 ppm_v), the hygrometer probe was found to have potentially serious errors consistent with earlier observations due to its relatively long response time and possible hysteresis [4]. Despite these difficulties the hygrometer probe appears to provide satisfactory calibration points for measurement of water vapor with the GC/MS at concentrations above about 10 ppm_v. More detailed information about these measurements will be given in our next quarterly report.

Measurement of the production rates of the oxyfluorides SOF_2 and SO_2F_2 from negative corona discharges in pressurized SF_6 have been extended to include the higher discharge power levels of 0.82 W, 2.22 W, and 4.29 W. The results are consistent with the trends discussed in our previous quarterly reports. It was observed also that even at these fairly high power levels the surfaces of the

point electrodes, after being subjected to continuous negative corona for many hours, exhibited very little in the way of deposits or pitting. This is in sharp contrast to the situation which generally prevails for positive corona discharges where extensive deposits and damage at the electrode tip are evident within a relatively short time (~1 h) when the discharge power approaches, or exceeds a level of about 1 W. This effect of polarity on electrode damage is perhaps to be expected on the basis of the known behavior of SF_6 corona [5].

The positive discharge current exhibits much more fluctuation than the negative discharge (see fig. 2) and tends to retain a pulsed characteristic even at relatively high currents; whereas, the negative discharge rapidly stabilizes and tends to behave like a steady glow discharge as the current increases. In the positive case the point electrode tip is evidently subjected to impact by many fast bursts of electrons from avalanches, or streamers formed in the gas. For the negative case, on the other hand, it is expected [5,6] that a space charge cloud develops around the point electrode thereby grading the field and reducing the energy of impacting ions. This appears to be consistent with the relatively stable current seen. It thus appears likely that the point electrode is heated more under positive discharge conditions, and the electrode surface possibly plays a greater role in the discharge chemistry. This effect may have some relevance to the observed polarity dependence for the ratio of SOF_2 and SO_2F_2 production rates (see tables 1 and 2). At present we can only speculate, but it is possible that free oxygen is more readily generated near the hot surface of the positive point; and since free oxygen is needed for SO_2F_2 production in the discharge [1,7-9], it might be expected, as observed, that this species is more readily produced in the positive case.

The GC/MS data have been reanalyzed to derive production rates for SOF_2 and SO_2F_2 expressed in terms of moles generated per unit of charge transported across the discharge gap, i.e., in moles-per-coulomb. The results of this analysis are tabulated in tables 1 and 2, respectively, for SOF_2 and SO_2F_2. Indicated in the tables are the corresponding discharge currents, power dissipations, and polarities as well as the gas pressures.

Examples of the data from which these rates were derived are shown in figures 3a-7a in which the measured concentrations of SOF_2 or SO_2F_2 in nanomoles are plotted versus the total accumulated charge Q transported across the discharge gap in coulombs. The net charge is computed from the discharge current I (held constant in these experiments) and the time t, using $Q = It$. The tabulated rates were obtained from fits to the GC/MS data of the form

$$C = B + AQ^{1+\varepsilon}, \tag{1}$$

where A, B, and ε are constants, and C is the concentration of the species of interest. From this the production rates are expressed as

$$\frac{dC}{dQ} = (1 + \varepsilon)AQ^{\varepsilon}. \tag{2}$$

The parameter B corresponds to initial concentration, usually below the limit of detection, and the parameter ε indicates the deviation from linearity. The solid lines in figures 3a-7a correspond to fits of the form given by eq (1).

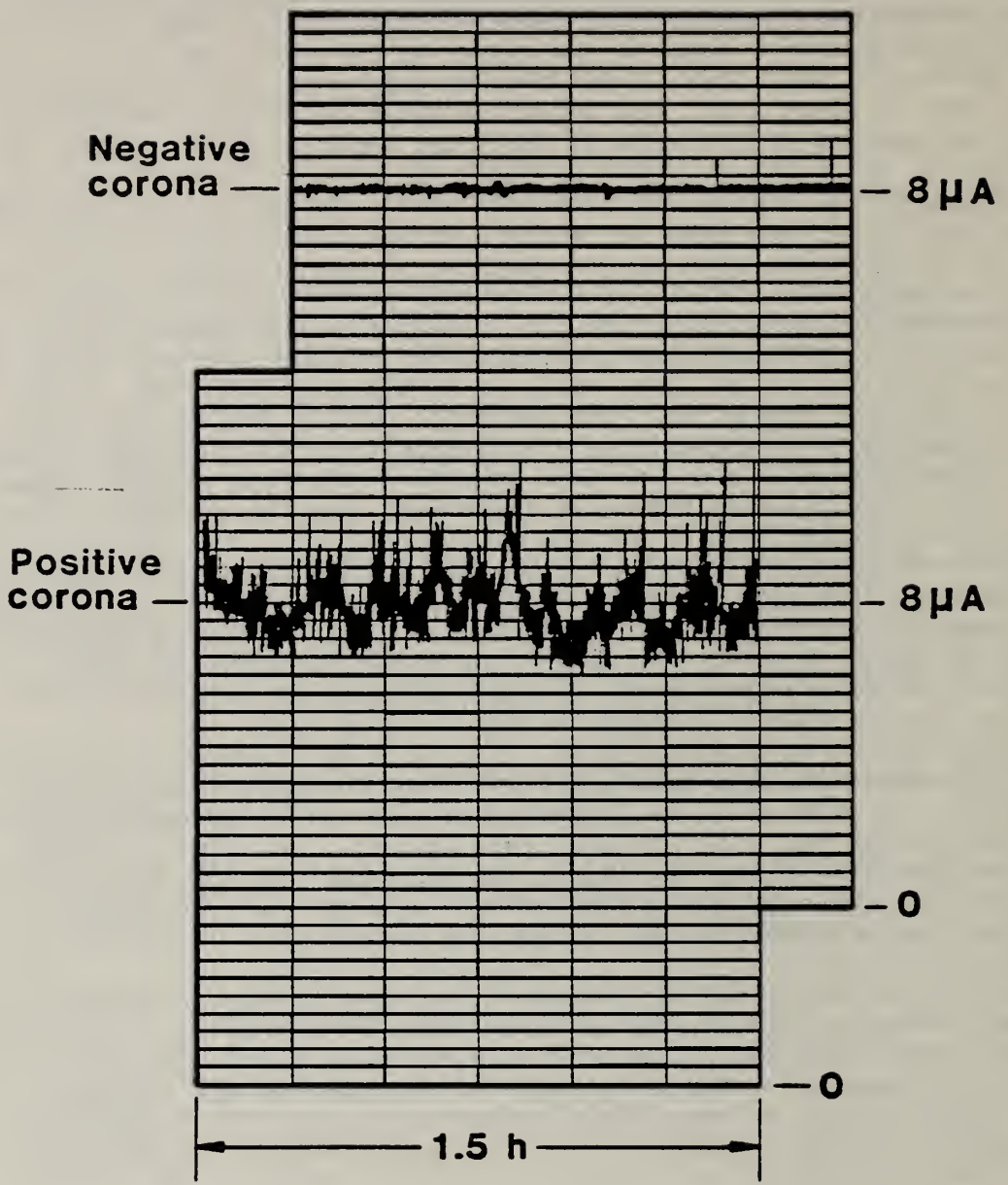

Figure 2. Recording of discharge current versus time for positive and negative corona in SF_6 at a pressure of 200 kPa. The average current in both cases is 8.0 μA.

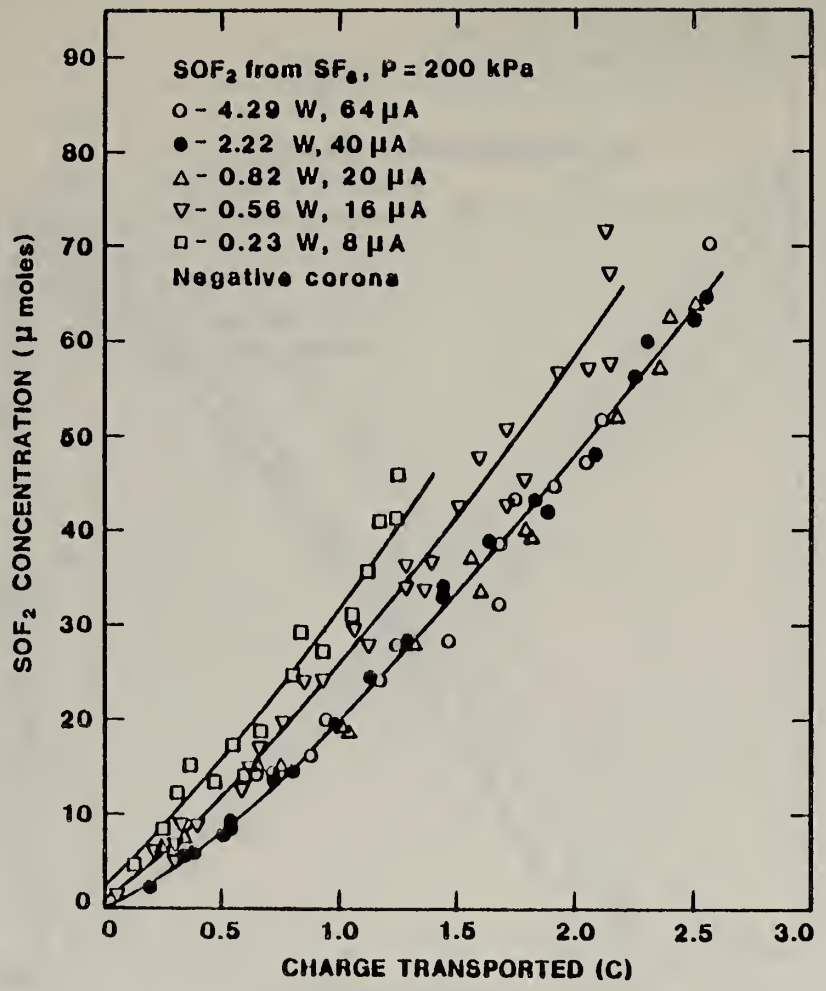

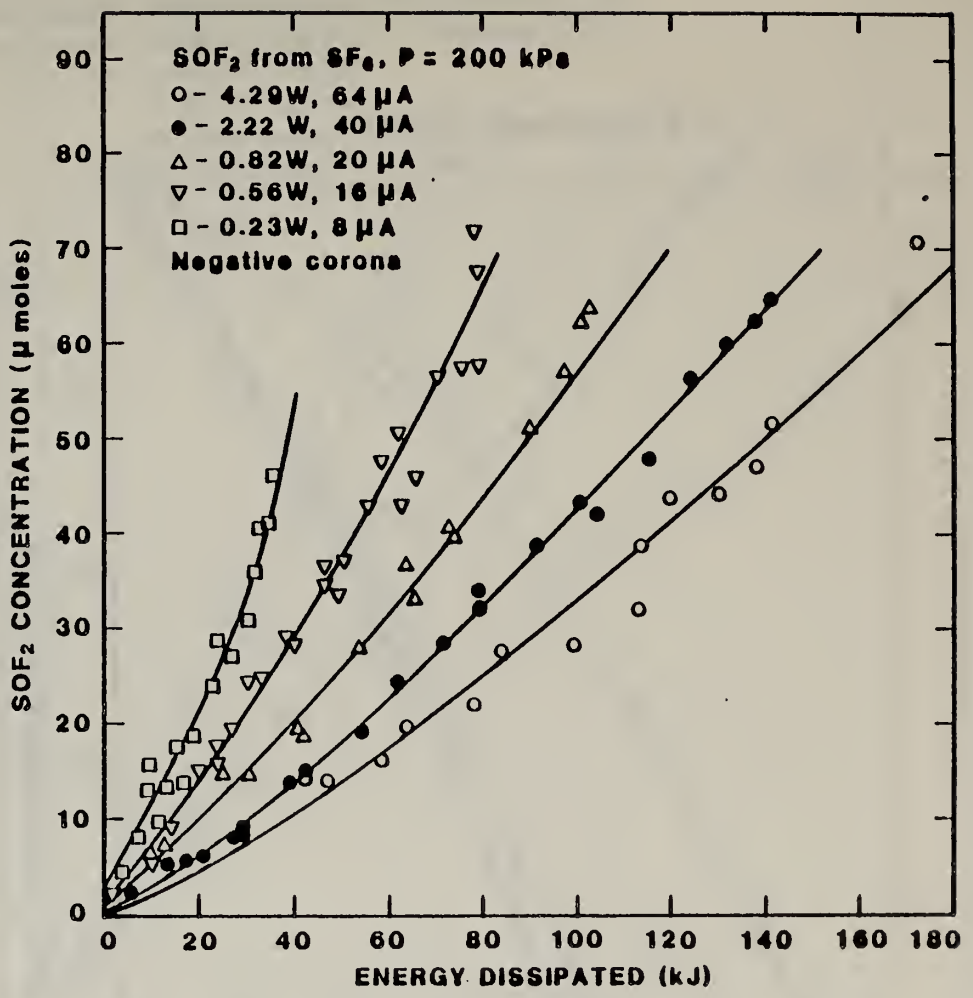

Figure 3. Measured concentrations of SOF_2 versus (a) net charge transported in the discharge gap, and (b) net energy dissipated in the discharge for negative corona in 200 kPa SF_6 at the indicated discharge powers and currents.

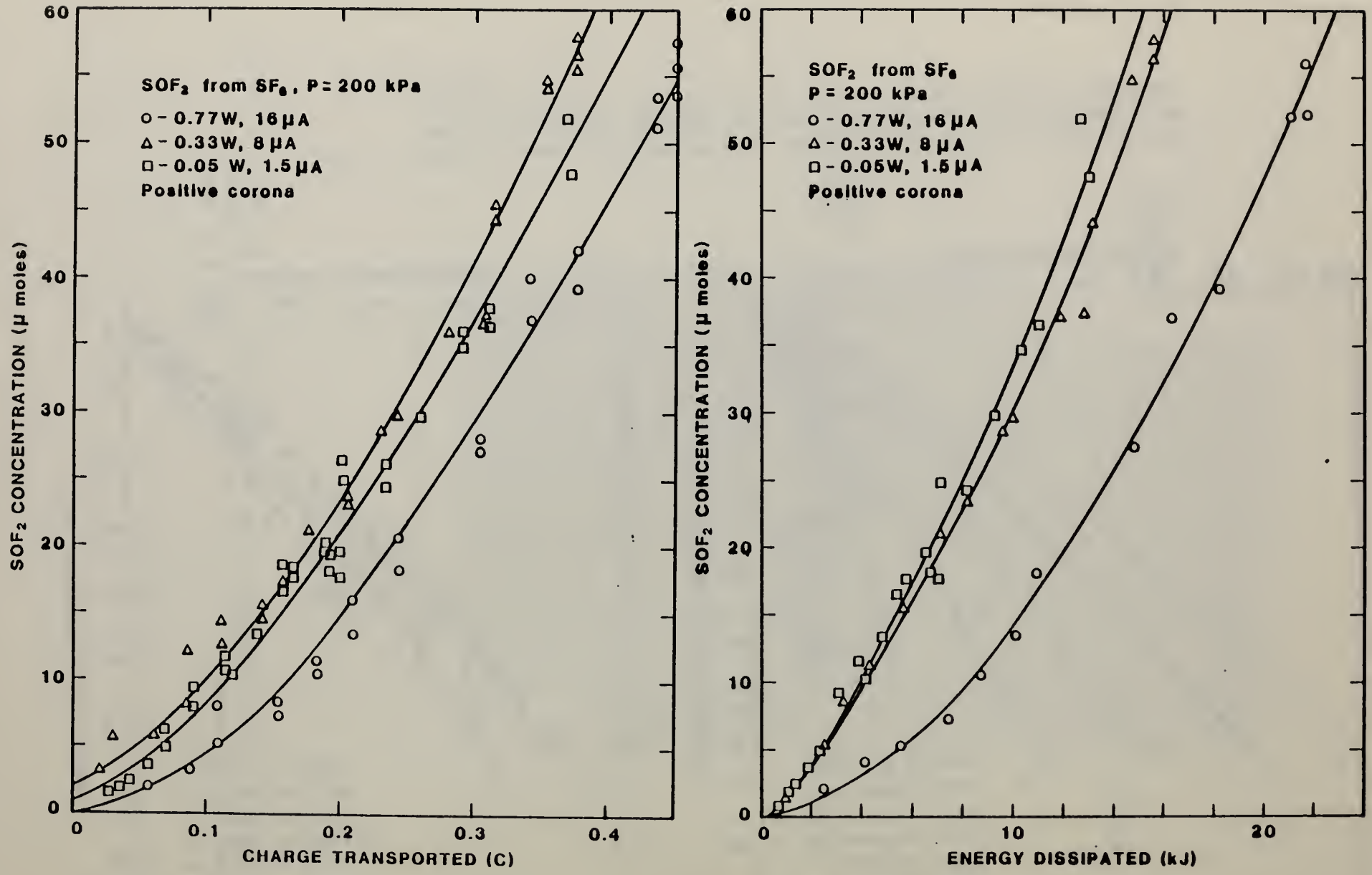

Figure 4. Measured concentrations of SOF_2 versus (a) net charge transported in the discharge gap, and (b) net energy dissipated in the discharge for positive corona in 200 kPa SF_6 at the indicated discharge powers and currents.

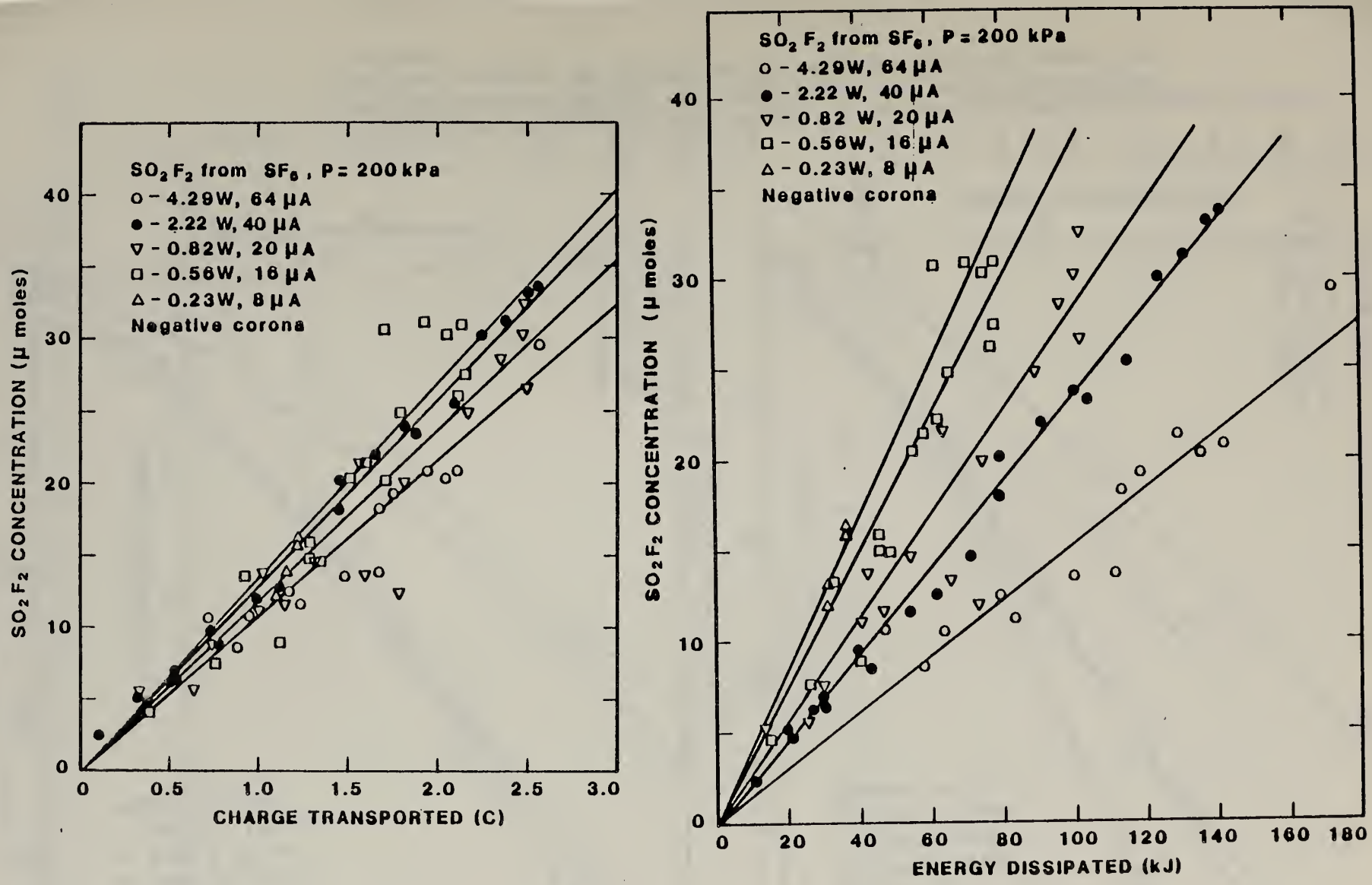

Figure 5. Measured concentrations of SO_2F_2 versus (a) net charge transported in the discharge gap, and (b) net energy dissipated in the discharge for negative corona in 200 kPa SF_6 at the indicated discharge powers and currents.

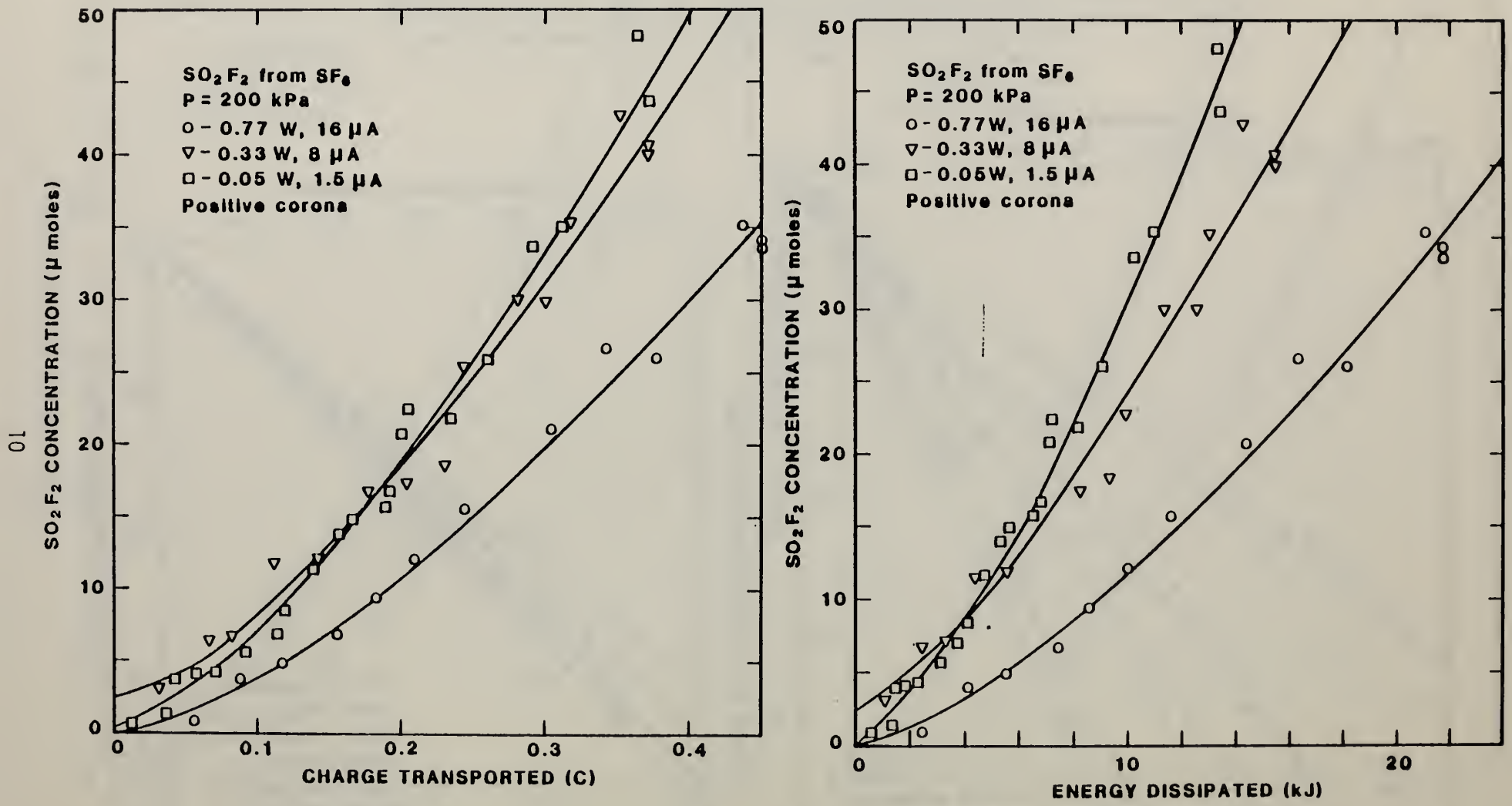

Figure 6. Measured concentrations of SO_2F_2 versus (a) net charge transported in the discharge gap, and (b) net energy dissipated in the discharge for positive corona in 200 kPa SF_6 at the indicated discharge powers and currents.

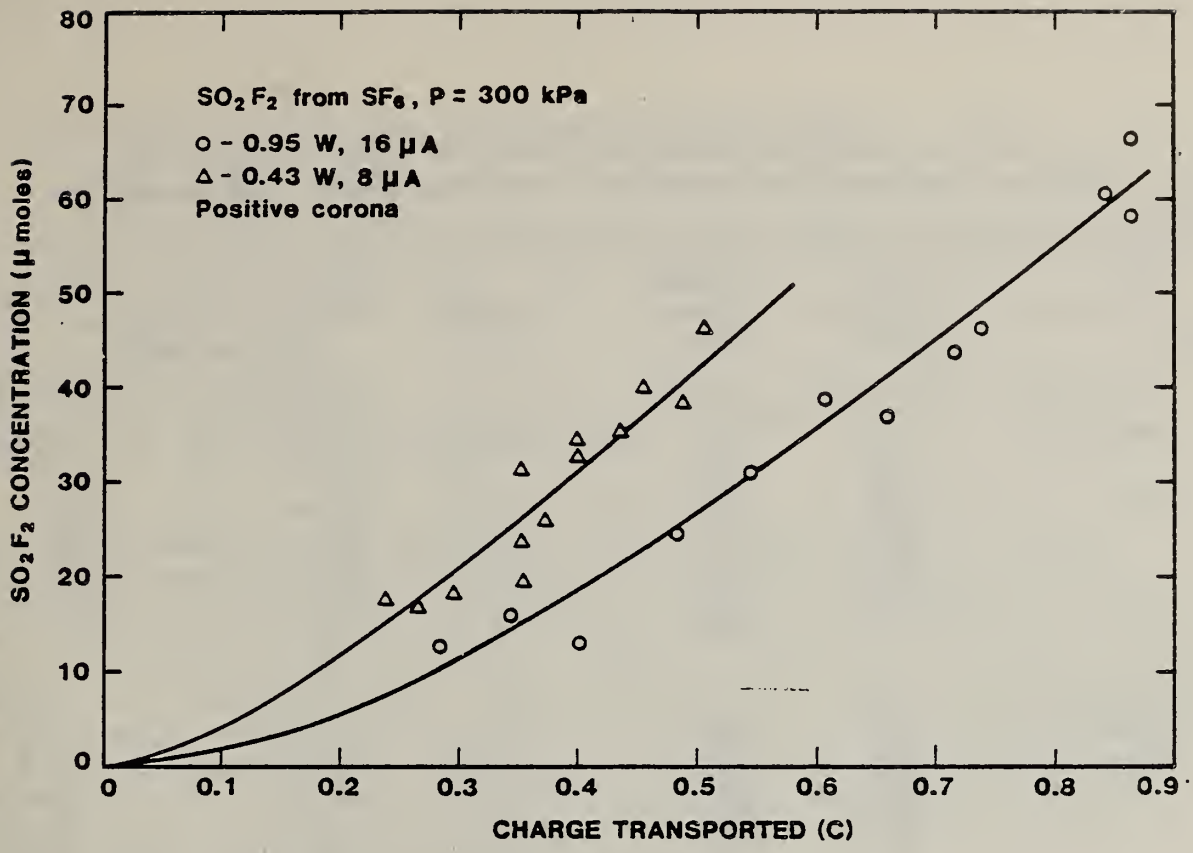

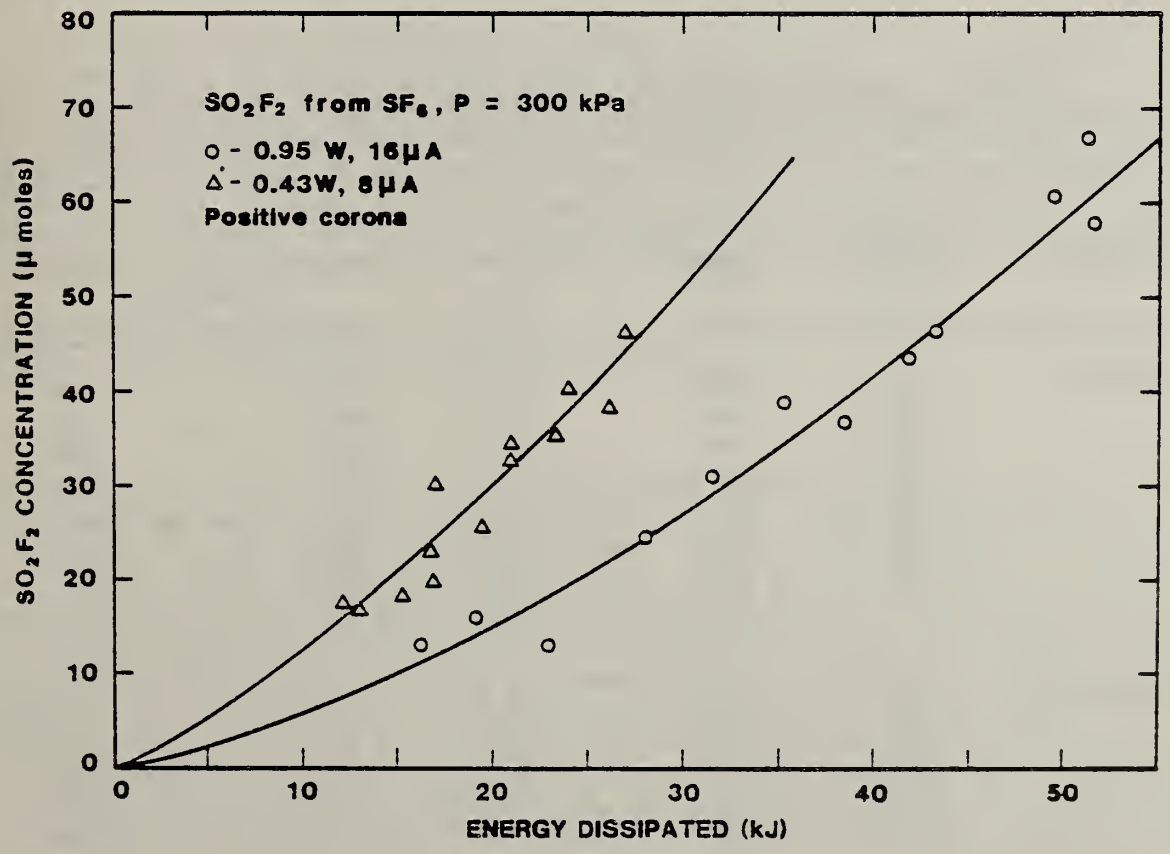

Figure 7. Measured concentrations of SO_2F_2 versus (a) net charge transported in the discharge gap, and (b) net energy dissipated in the discharge for positive corona in 300 kPa SF_6 at the indicated discharge powers and currents.

Table 1. Measured production rates for SOF_2 in SF_6 at the different indicated gas pressures, discharge powers, and polarities.

Polarity	Gas Pressure (kPa)	Average Power (mW)	Current (μA)	Measured Production Rates (n moles/C) Q = 0.3 C	Q = 0.4 C
Positive	116	804	20.0	18.2	21.6
	200	54	1.5	172	198
	200	335	8.0	189	221
	200	777	16.0	159	200
	300	198	4.0	204	298
	300	430	8.0	142	172
	300	945	16.0	89	109
Negative	200	230	8.0	25.4	27.8
	200	586	16.0	23.0	24.6
	200	821	20.0	21.5	22.0
	200	2215	40.0	19.0	20.2
	200	4290	64.0	18.7	20.0

Table 2. Measured production rates for SO_2F_2 in SF_6 at the different indicated gas pressures, discharge powers, and polarities.

Polarity	Gas Pressure (kPa)	Average Power (mW)	Current (μA)	Measured Production Rates (n moles/C) Q = 0.3 C	Q = 0.4 C
Positive	116	804	20.0	24.0	28.5
	200	54	1.5	162	188
	200	154	4.0	176	208
	200	335	8.0	136	158
	200	777	16.0	94	109
	300	198	4.0	105	125
	300	430	8.0	100	112
	300	945	16.0	60	71
Negative	200	230	8.0	5.4	7.4
	200	586	16.0	10.1	11.9
	200	821	20.0	11.3	11.4
	200	2215	40.0	9.7	10.3
	200	4290	64.0	11.0	10.7

The production rates per-unit-time can be found using

$$\frac{dC}{dt} = I \frac{dC}{dQ} , \tag{3}$$

or, if the production rates are expressed in terms of moles-per-unit of energy U dissipated in the discharge, then

$$\frac{dC}{dt} = p(t) \frac{dC}{dU} , \tag{4}$$

where p(t) is the discharge power, which was, in general, slightly time dependent for the experiments reported here.

Figures 3b-7b show plots of the concentration C versus the energy U from which the production rates expressed in terms of moles-per-unit of energy dissipated given in our previous quarterly report were obtained. It is significant to point out that the production rates given by (dC/dQ) show much less variation with discharge power (or equivalently current) than rates defined as (dC/dU). In fact, as figures 3b-7b indicate, (dC/dU) tends on the average to decrease with increasing power, whereas (dC/dQ) shows in most cases only a small variation with current, which in view of the uncertainties in the measurements is of doubtful significance. Therefore, we can conclude from the measurements performed to date that the time-rates of production, (dC/dt), of the species SOF_2 and SO_2F_2 in both positive and negative corona discharges are nearly directly proportional to the discharge current I.

This conclusion is supported by a direct comparison of the C versus Q data in figures 3a-7a with the C versus U data in figures 3b-7b. It should be noted that although the trend suggesting that $(dC/dt) \propto I$ is evident for both positive and negative discharges, the results for the negative case must be considered more reliable because, as the data in figure 2 would indicate, the average discharge current is more accurately measured and controlled during the negative discharge. The data in figure 2 correspond to a time interval of 1.5 h for 8 μA discharges in SF_6 at a pressure of 200 kPa for positive and negative polarities.

If the formation of the observed stable oxyfluoride species involves an electron-induced dissociation reaction such as

$$e + SF_6 \rightarrow SF_4 + 2F + e \tag{5}$$

as the initial step, then it can be argued that their production rates should be nearly proportional to I, since the rate of initial dissociations will be proportional to the number of electrons which pass through the gas in a given time, provided that they possess sufficinet energy to induce dissociation. Of course it can be objected that, if the discharge current is varied for a given gas pressure and gap configuration, it is necessary to change the electric field in the gap as well, and thus also, the mean translational kinetic energy of the electros. This would in turn affect the probability for the occurence of reactions such as that of eq (5) above. Although admittedly this could give rise to an increase (or decrease) in (dC/dQ) with discharge current, there is reason to believe that this effect should be relatively small. It is known [10] that at high field-to-gas density ratios, E/N, where ionization in the gas becomes quite probable, typical electron excitation coefficients, including dissociation and dissassociative excitation, show only slow variations with E/N. This is because the cross sections for processes such as eq (5) above

usually tend to level off and eventually slowly decrease with increasing mean electron energy. This consideration, together with the expectation that as current increases so will the space charge in the gap which tends to moderate E/N near the point electrode, leads one to suspect that variations in the production rates (dC/dQ) with discharge power will be generally small. It should also be kept in mind that the production of oxyfluorides is also influenced by external factors such as the concentrations of oxygen and H_2O, and these may be affected by the discharge power level.

The results presented here suggest that it may be preferable to express production rates of discharge-generated gaseous by-products in terms of concentration-per-unit of charge transported, rather than per unit of energy dissipated. This choice is also more convenent from a practical point-of-view, since discharge current is more easily and accurately measured than power dissipated. Also, it allows a more meaningful application of the data to situations where there may be time varying voltages, e.g., 60 Hz ac conditions.

During the next quarter, more measurements will be made of oxyfluoride production rates from corona in SF_6 and SF_6/H_2O mixtures. The emphasis will be on attempting to understand the effects of water vapor, and the factors that influence the equilibrium concentration of water vapor during a corona discharge. Measurements will be performed to evaluate the response time of a thin-film aluminum oxide hygrometer probe for measurement of H_2O in SF_6 and to determine the uncertainties in the use of this device to calibrate the GC/MS for H_2O measurements. It is expected that the first quantitative determination will be the H_2O consumption or production during discharge operation in SF_6.

For further information contact Dr. R. J. Van Brunt, (301) 921-3121, National Bureau of Standards, Washington, DC.

4. OPTICAL MEASUREMENTS FOR INTERFACIAL CONDUCTION AND BREAKDOWN IN INSULATING SYSTEMS
Subtask No. 04

The objectives of this investigation are to develop apparatus and appropriate procedures for the optical measurements of interfacial electric field and space-charge density in materials for electric power equipment and systems, to understand the interfacial pre-breakdown and breakdown of processes in specific insulating systems, and to demonstrate the applicability of the developed instrumentation and the methodology in the development and design of future systems.

During the previous quarter, measurements were made of the Kerr coefficient of transformer oil as a function of the wavelength of the probing light. The determination was made over the visible spectrum and for two temperatures, 24°C and 97°C. The results demonstrated that the variation was small, so that there was no need to pursue that topic further for the present.

Using dc voltage and a pressboard interface parallel to the field, for example, it is observed that breakdown occurs around 40 kV/cm, whereas without an interface, the strength of the oil alone is around 90 kV/cm. This situation suggests the question: Is the lowered breakdown voltage of the interfacial system due to space charge field enhancements which are present and cannot easily be measured, or is space charge not detected because it is insufficient

to modify the electric field? The question of onset of space charge and the temperature dependence of the nonuniformity of the electric field (field enhancement) is settled this quarter to a great extent. Further, some light is shed on the possible origins of space charge.

A sample of transformer oil is subjected to the field between parallel plates so that the spatial dependence of the electric field can be measured using the electro-optical Kerr effect. If space charge is not present, then the field between the plates is uniform. Let the uniform field strength be denoted $E_{ave} = V/d$ where V is the applied voltage and d is the plate separation (in this case d = 0.64 cm). As discussed in earlier reports, the light transmitted through the cell due to the Kerr effect is given by

$$I(z)/I_m = \sin^2(\pi/2)[E(z)/E_m]^2, \tag{6}$$

where z denotes the distance from anode to cathode, E is the electric field, $E_m = V_m/d$ where V_m is the cell constant (voltage for full transmittance), I_m is the incident intensity and I is the transmitted intensity. Because the Kerr effect in transformer oil is small, the following approximation is quite accurate:

$$I(z)/I_m = (\pi/2)^2[E(z)/E_m]^4 . \tag{7}$$

If there is no space charge, then an amount of light I_{ave} will be transmitted through the cell which corresponds to the average field E_{ave}. If the incident intensity I_m is uniform then I_{ave} will be uniform. Usually, it is rather simple to arrange for a relatively uniform incident light intensity, at least for the accuracy needed here -- about 5%.

The field nonuniformity (or enhancement as it is sometimes called) which arises from space charge in the oil is best characterized by examining the relative field. That is, rather than determining the ratio $E(z)/E_m$, the ratio of the field to what it would be if space charge were not present is more meaningful, $E(z)/E_{ave}$. Such a representation of the field aids one to think in terms of percent field enhancements. Using eq (7) the relative field is given by

$$E(z)/E_{ave} = [I(z)/I_{ave}]^{(1/4)}. \tag{8}$$

By integrating eq (8) I_{ave} can be related to an integral of the light intensity as

$$(I_{ave})^{(1/4)} = (1/d) \int [I(z)]^{1/4} dz, \tag{9}$$

which is just the average of the fourth root of the light intensity profile between the plates. This method works well only if the incident light intensity is relatively uniform. A much more extensive analysis is necessary whenever the incident light is not sufficiently uniform, for then $I_m(z)$ must be measured for each I(z).

Throughout this investigation dc voltages are applied. A determination of the relative field is made for each polarity. The space charge is negative and tends to increase its concentration from nearly zero in the vicinity of the cathode to its maximum value (of order 200-300 pC/cm^3) next to the anode. The

maximum relative field nonuniformity is measured for each polarity and the average used is to characterize the field nonuniformity at a given voltage and temperature. A plot of the maximum relative field nonuniformity as a function of temperature and applied field is shown in figure 8.

There are two aspects of the data which should be highlighted because of their potential significance. First, the space charge content appears to have an onset which decreases as the temperature increases. This would explain why no field enhancements were observed in the vicinity of an interface during previous investigations -- the breakdown field strength was not sufficiently strong to initiate space charge. Second, there may be a saturation of space charge at the higher temperatures and fields. However, because of the uncertainty of these data, further research must be carried out to test this hypothesis.

In an attempt to identify the origin of the space charge, two additional sets of measurements were performed. First, to test the hypothesis that the space charge is due to water, the water was removed from the oil. Specifically, oil at 122°C, in which the field distortion was approximately 30%, was filtered through activated alumina. The filtered oil exhibited no field distortion. If water is then added to the oil, however, the field distortion remains negligibly small. So, water alone is probably not the origin of the space charge.

The second hypothesis tested was the suggestion that the space charge was the result of particulate contamination. This was done by adding 5 mg of carbon particles (with a distribution of diameters which was probably peaked in the 1-10 μm range) to 2.8 liters of oil. Again, no space charge was produced.

It is anticipated that much of the construction of the interfacial breakdown cell will be finished during the next quarter. Its purpose is to provide a means to change the interface in a high-temperature cell without opening the cell. The resultant breakdown information -- with and without an interface -- as a function of temperature will be useful in modeling phenomena in practical systems, especially if the space charge in the oil can be monitored and controlled.

The International Conference on Interfacial Phenomena will be held in late September. All authors have been contacted and a tentative agenda will be developed early next quarter.

For further information contact Dr. Edward F. Kelley, (301) 921-3121, National Bureau of Standards, Washington, DC.

5. ACTIVE INSULATORS FOR INSULATION AND SURGE SUPPRESSION
Subtask No. 04

This section of the quarterly report describes the work performed by the Electrical Engineering Department of the University of Southern California under a grant from NBS to evaluate the concept of active insulators. These insulators are to be built with a nonlinear voltage dependent resistance, which is designed to reduce the effects of switching and lightning surges.

The project consists of two parts: first, a theoretical part to develop a mathematical model to predict the behavior of active insulators on a

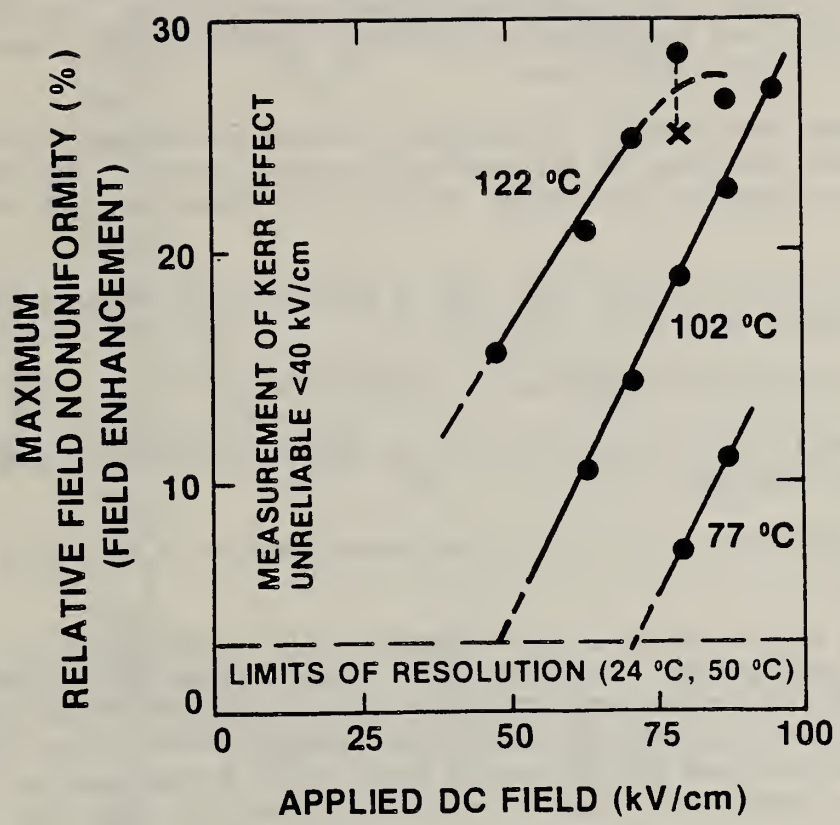

Figure 8. Maximum field enhancement in percent as a function of applied dc field for various temperatures. The field is enhanced nearest the anode indicating a negative space-charge density. Measurable field nonuniformities could not be found for temperatures below 50°C before breakdown field levels were reached near 90 kV/cm. Data taken were insufficient to determine the cause of the apparent leveling off of the enhancement for the 122°C measurements, however, the data point marked with "x" indicates a reduction of space charge may have occurred overnight. Because of the "noise" in the data and imperfections in the optics, resolution was limited, and reliable field measurements could only be made for fields over 40 kV/cm.

transmission line; and second, an experimental part to install a materials research facility to fabricate and evaluate simple prototype insulators.

During this quarter the simulation program based on the algorithm described in the previous quarterly report was implemented on a computer to model three-phase systems under conditions of switching surges. The materials laboratory setup was completed and the formulations tested showed significant improvement, as described below.

The model developed to represent a three-phase transmission line during transients was described in the previous progress report. The model has been validated by comparing calculation results with those reported in the literature.

In this study a 240 km long, 345 kV transmission line was simulated under three switching conditions:

1. Energizing an open line.

2. Energizing an open line with one phase shorted to ground at the receiving end.

3. Re-energizing a line with one phase shorted to ground at the receiving end.

Figures 9, 10, and 11 show the maximum voltage waveforms for the three conditions, respectively. In each figure, part (a) is the voltage waveform calculated at the sending end; part (b), at the midpoint of the line; and part (c), at the receiving end. The solid line refers to the case without nonlinear insulators on the line and the dotted line refers to the case for which 10 nonlinear insulators were evenly distributed along the same line (per phase).

The above figures clearly indicate that the installation of nonlinear insulators reduces the overvoltage magnitudes for all three conditions.

Figures 12, 13, and 14 illustrate how the maximum overvoltages are reduced and how the voltage is more evenly distributed along the entire length of the line when nonlinear insulators are used. These figures also show the strong effect the parameter α of the nonlinear impedance material has on the resulting overvoltages.

The effect of the number of installed nonlinear insulators on the overvoltage magnitudes and distribution can be seen in figures 15 and 16. If a total of only 30 nonlinear insulators are installed (one per phase every 24 km in this study), an almost uniform distribution can be obtained for the 240 km line.

Power dissipation during the transient by the nonlinear insulators is a primary consideration in the application of these devices, and it was also investigated. It was found that for the case of energizing the system with one phase-to-ground, the energy which a nonlinear insulator unit must handle is 54 kWs, or 24% of the energy a station arrester must dissipate on a line without nonlinear insulators. During re-energization, a nonlinear insulator unit

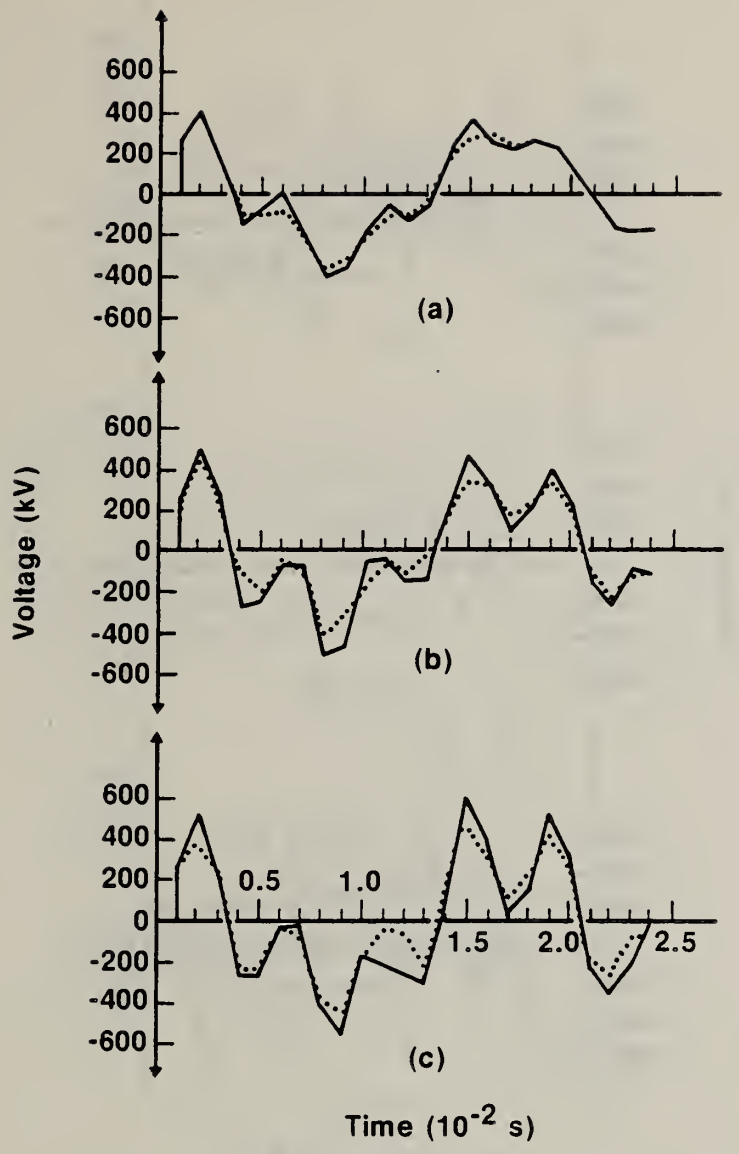

Figure 9. The overvoltage waveform during condition 1.

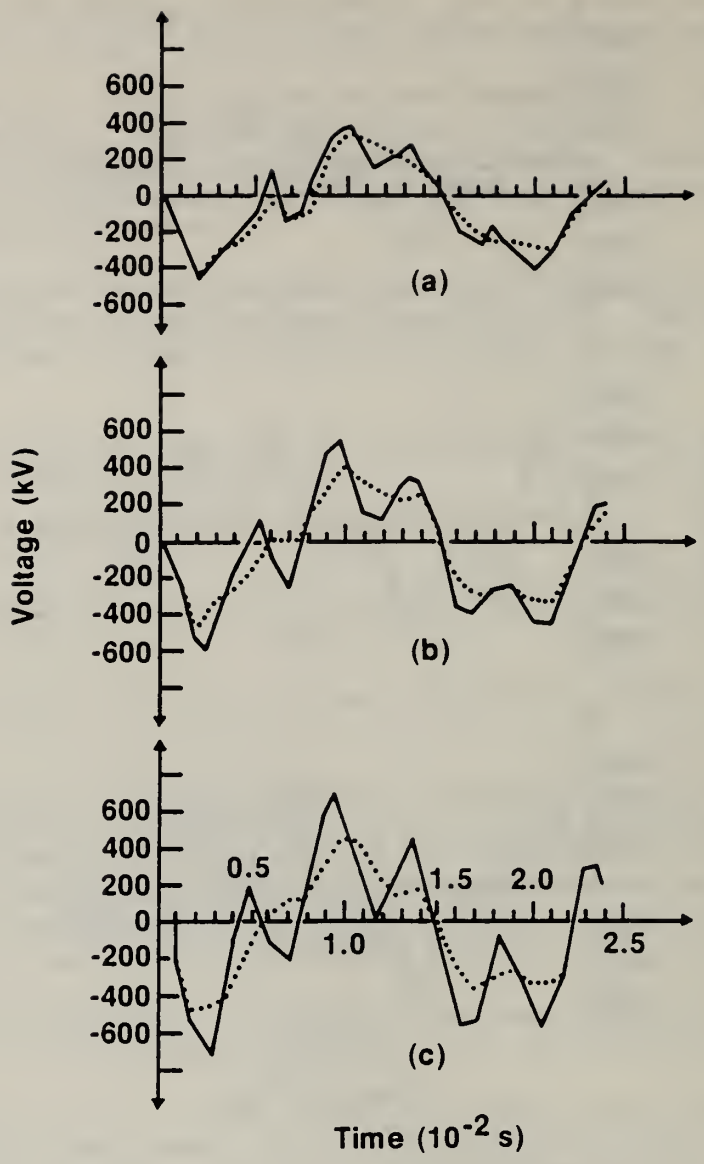

Figure 10. The overvoltage waveform during condition 2.

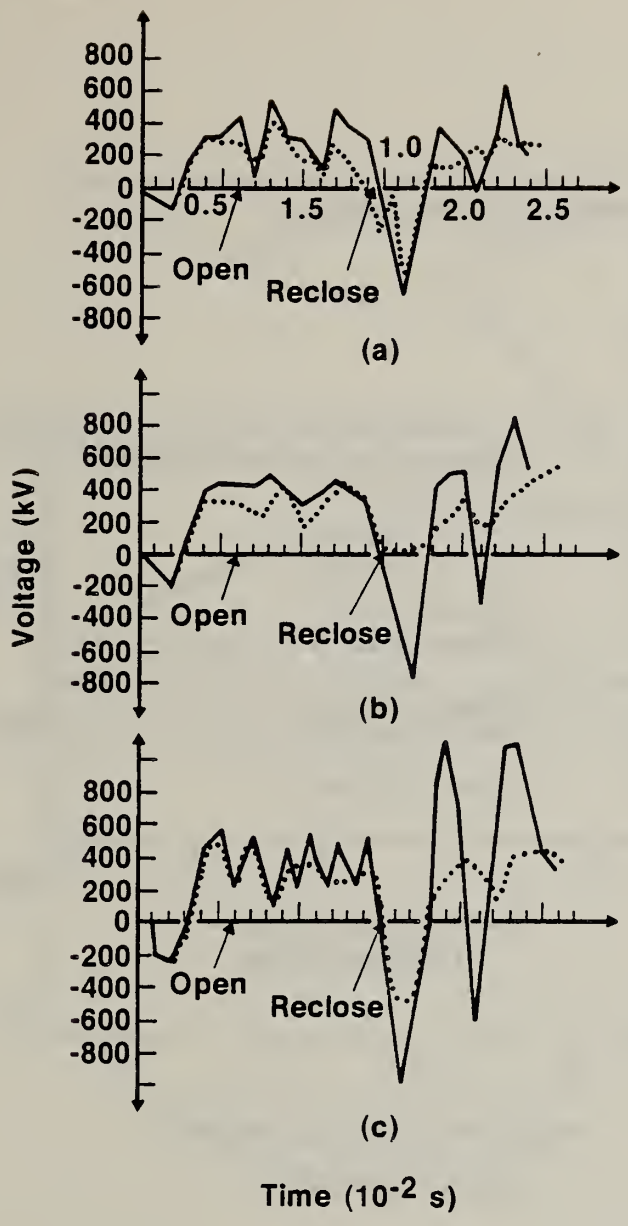

Figure 11. The overvoltage waveform during condition 3.

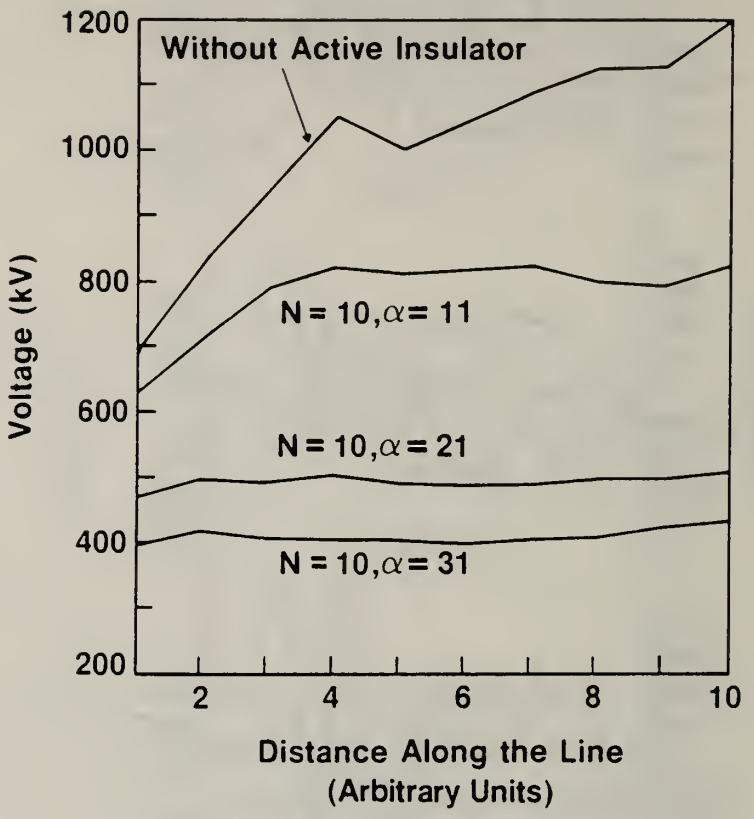

Figure 12. The distribution of maximum overvoltage along the line during condition 3.

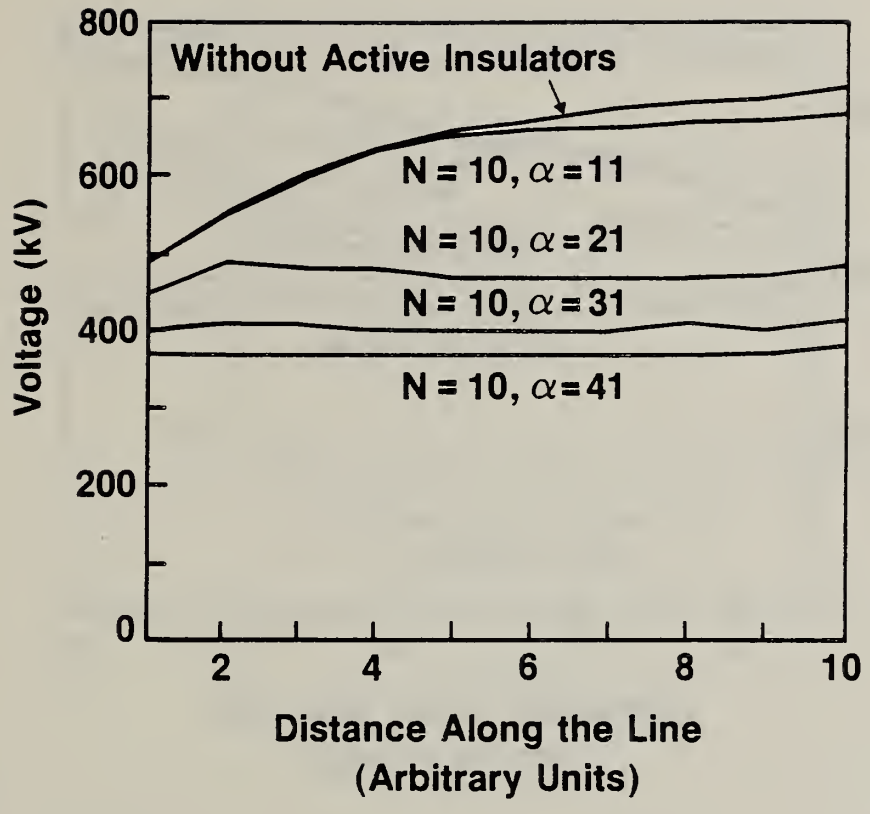

Figure 13. The distribution of maximum overvoltage along the line during condition 2.

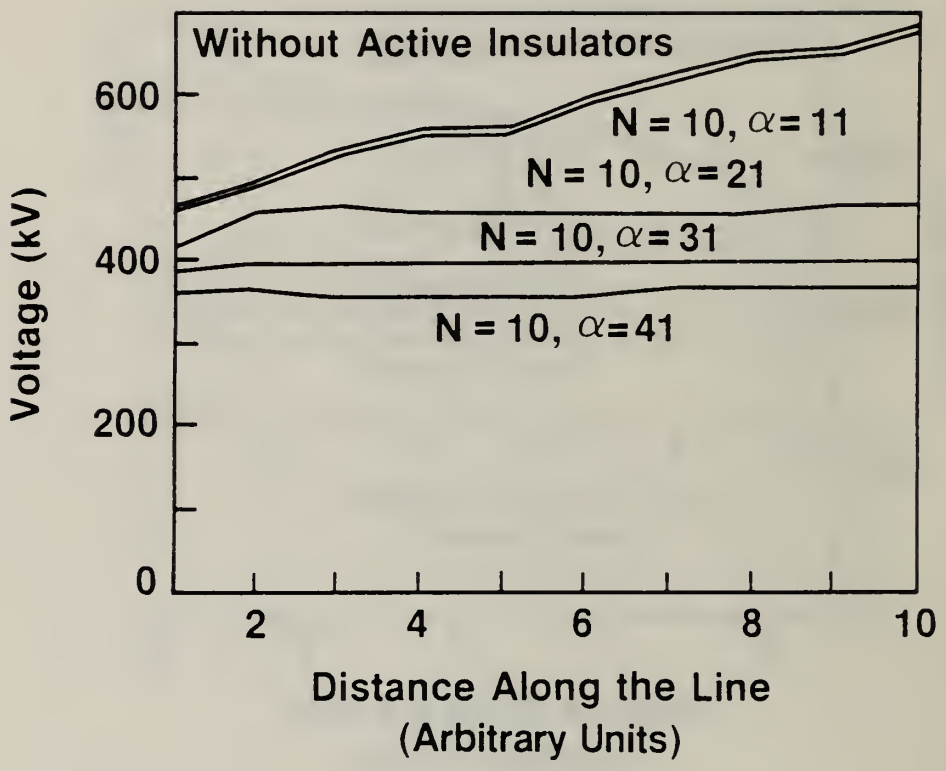

Figure 14. The distribution of maximum overvoltage along the line during condition 1.

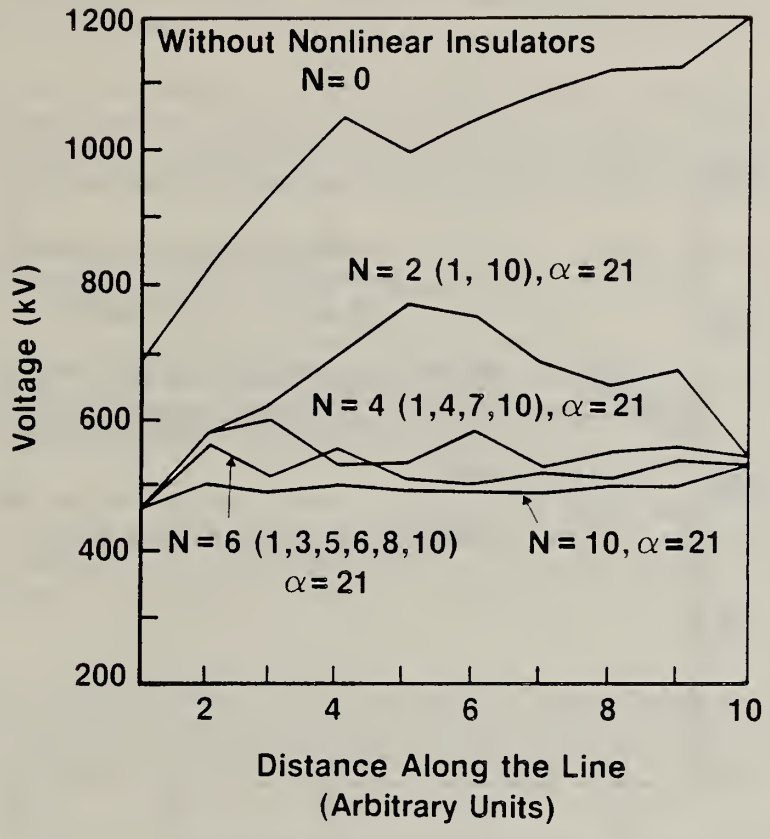

Figure 15. The effect of the number of nonlinear insulators installed on the distribution of maximum overvoltage during condition 3.

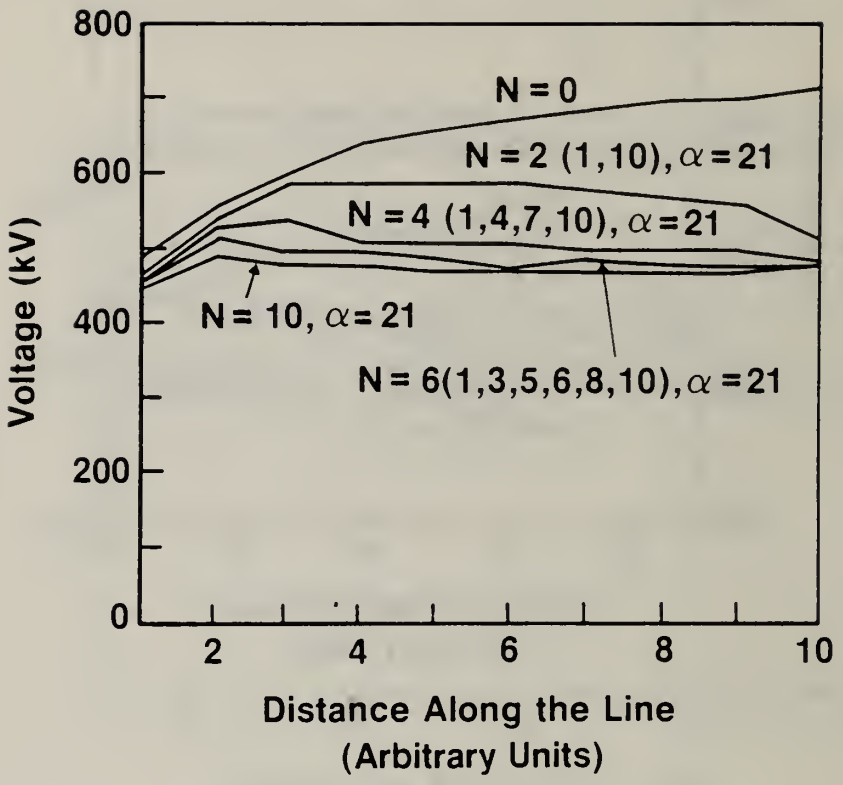

Figure 16. The effect of the number of nonlinear insulators installed on the distribution of maximum overvoltage during condition 2.

handles 130 kWs, or 20% of the energy a station arrester must dissipate when only conventional insulators are used. Figures 10 and 11 graphically illustrate how the thermal duty of a station arrester is reduced with nonlinear insulators.

From this theoretical study, three preliminary conclusions of practical importance can be derived:

1. Nonlinear insulators can effectively limit overvoltage magnitudes along the entire length of transmission line, requiring the installation of relatively few of these special devices (at towers every 24 km for the 240 km line in this study).

2. The energy which the nonlinear insulators must dissipate is in accordance with the present zinc-oxide technology, at least on a short-term basis.

3. With nonlinear insulators the insulation level of the system can be reduced to a point where transient overvoltages are no longer a principal consideration in this regard.

During this period, discs, rods, and tensile test samples were prepared in the materials research facility. Electrical and mechanical tests show that the mechanical properties of the polymer concrete could be improved without degrading the electrical characteristics. The test results obtained appear in table 3.

Future work in this area consists mainly in developing molding and coating techniques to be able to fabricate simple nonlinear insulators. These prototype insulators will be used in the experimental evaluation of the nonlinear insulator concept.

Table 3. Electrical and mechanical properties of polymer concrete samples.

	Average	Best
Loss Tan δ	~ 0.04	0.017
Dielectric constant	~ 3.5	1.7
Volume resistivity (ohm/cm)	~ 0.6×10^{15}	1.15×10^{15}
Dielectric breakdown kV/mm	~16.0	~20.0
Compression strength Pa	~1.8×10^{8}	2.14×10^{8}
Tensile strength Pa	~ 2.2×10^{7}	2.44×10^{7}

For further information contact Dr. T. C. Cheng, (213) 743-6938, University of Southern California, Los Angeles, CA.

6. INVESTIGATION OF INSULATOR SURFACE FLASHOVER IN GAS
Subtask No. 04

The objectives of this research, which is being carried out at the University of South Carolina, are to determine the basic mechanisms leading to insulator surface flashover in gas and to determine the roles of various, controllable parameters in the flashover process. It has been previously postulated that insulator surface charging, surface fields, and surface currents are important in flashover production. Diagnostics have therefore been developed and have been used to measure insulator surface currents and fields, prior to breakdown, for different materials and geometries. Additionally, analytical techniques are being developed to analyze and assist in the understanding of the data produced. Accomplishments made this quarter and tasks to be performed during the next quarter are presented in this report.

Accomplishments made during this quarter include: (1) measurement of breakdown voltage and current, in gas along polymethylmethacrylate (PMMA) insulators of various shapes, surface conditions, and geometries; (2) continued modification of the electro-optical experimental arrangement; (3) a field analysis computer code obtained from NBS has been made operational; and (4) models are being fabricated to enable use of the electrolytic tank for field analyses.

The breakdown voltage and surface currents have been measured along PMMA insulators, using previously developed diagnostics. Results show the effect of insulator surface angle A, surface roughness, and voids (along the insulator and at the triple junction). Figure 16 shows the insulator breakdown (flashover) voltage, V_{bd}, in nitrogen, as a function of pressure p, for various angles. The electrode separation is maintained at 5 mm. The angle A is defined to be the angle between the applied field (normal to the electrode surface) and a normal to the insulator surface. It can be observed that: (1) V_{bd} increases approximately linearly with p; (2) V_{bd} (90 degrees) > V_{bd} (60 degrees) > V_{bd} (15 degrees), i.e., V_{bd} decreases as the angle decreases and the insulator becomes "flatter."

It should be noted that this behavior is very different from that observed for pulsed voltages in vacuum, where V_{bd} increases markedly as A varies from 90 degrees to 45 degrees. It should be further noted that V_{bd} increases for larger A even though the effective path length along the insulator increases with larger A. It can be postulated that the observed decrease in V_{bd} with A is due to the increase in the surface fields in gas at the acute angle between the insulator and electrode surfaces, for A less than 90 degrees, and/or the increased insulator surface area and triple junction length for smaller A values. The observed performance is significant, since it implies that high pressure gas insulators should be designed with large A values.

Similar data have been obtained using SF_6 instead of nitrogen. The results show a performance similar to that of figure 17 except all voltages are higher by a factor of 2.5.

Regarding the data of figure 17, it has also been observed that $V_{bd}(A)$ for a rough surface (sandblasted) is slightly less than for a polished surface. The performance is, however, more repeatable and predictable. Additionally, it has been observed that the flashover along polished PMMA is constricted and

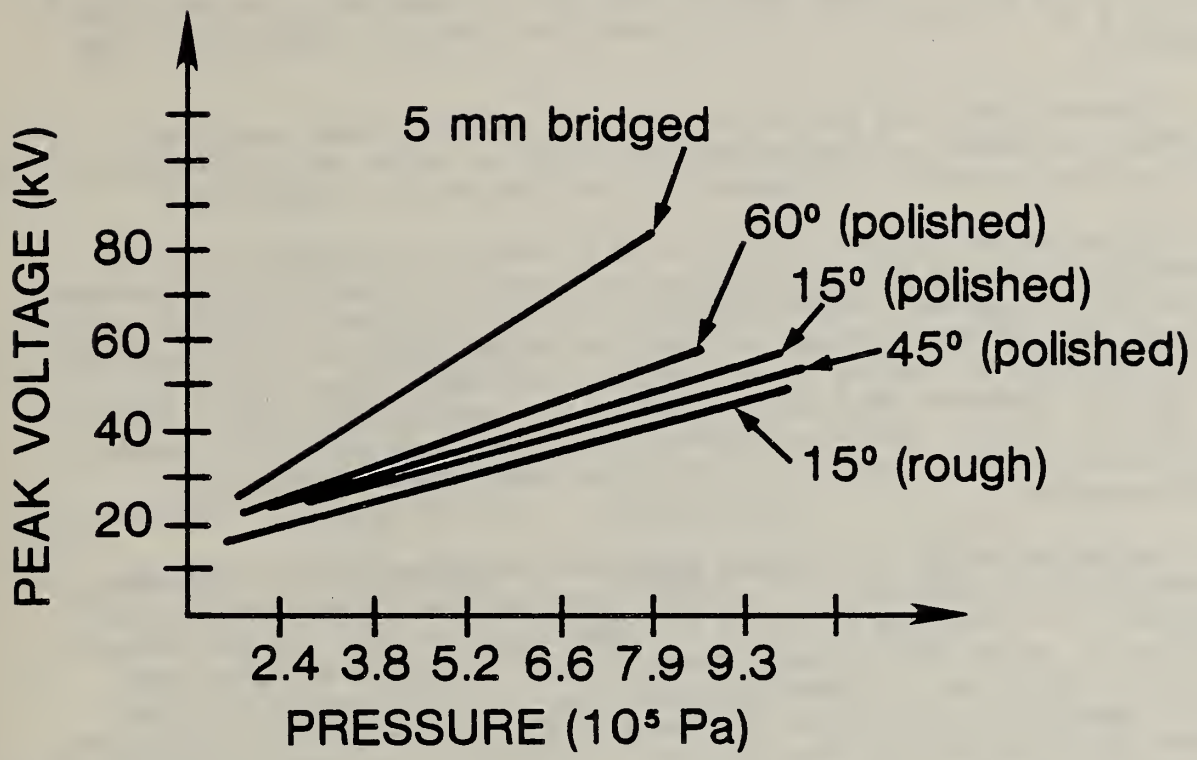

Figure 17. Breakdown voltages for various cone angles.

ultimately causes a track. The discharge is, however, diffuse along the roughened surface. This last observation implies that roughened insulator lifetime may exceed that of polished (or smooth surfaced) insulators.

It has been further observed that the flashover luminosity, during conduction, is away from the insulator for $1.73 \times 10^5 < p < 4.5 \times 10^5$ Pa and along the surface for $p > 4.5 \times 10^5$ Pa.

Surface currents (partial discharges), i, have also been measured as a function of A and p. These results show that no measurable current flows for $p < 5.5 \times 10^5$ Pa. Small surface currents are, however, measured for high pressures.

Breakdown data and surface current data have also been obtained to determine the effect of triple junction voids and voids (or imperfections) along the insulator surface. The geometries test are shown in figure 18.

The values of V_{bd}, as a function of p, have been determined for the geometries of figure 18(a) and (c) and are shown in figure 19, together with values for the surface current inception voltage, V_i, the current extension voltage, V_e, and the breakdown voltage for an unbridged gap. The data show that: (1) V_{bd}, V_i, and V_e are all linearly increasing functions of p; (2) V_{bd} for the unabridged and bridged gap are approximately equal, up to 1×10^6 Pa; (3) V_{bd}, with the void (as shown in figure 18(c)), is lower than V_{bd} without the void; and (4) V_i and V_e are both linearly increasing functions of p.

The values of V_{bd} for all the geometries of figure 18 have also been determined for vacuum and 1.73×10^5 Pa nitrogen, for comparison purposes. These data are indicated in figure 18, where V_{bdv} and V_{bdn} are the breakdown voltages in vacuum and nitrogen, respectively. It should be noted that: (1) $V_{bdv} > V_{bdn}$, for all geometries; (2) V_{bdv} is approximately the same for all geometries except that of figure 18(d); the presence of a total gap between the insulator and the electrode, therefore, considerably degrades (by a factor of 2) the hold-off performance; (3) the presence of a perturbation on the insulator does not degrade V_{bdv} or V_{bdn}; and (4) the presence of a partial gap, as in figure 18(c), substantially degrades V_{bdv} but not V_{bdn}. This implies that the gas in the void, where there is considerable field enhancement, due to the lower gas permittivity, is ionized by a lower, total applied voltage. It further implies that field emission in the high field, vacuum gap region does not greatly lower V_{bdv}. Particularly, these results show that voids at the triple function substantially decrease V_{bd} for gas and should certainly be eliminated in high voltage designs.

It should be noted that non-zero surface current has been measured in nitrogen for the geometries of figure 18(c) and (d). This implies that the presence of a void, near the electrode, produces partial discharges in the gas void. It is further postulated that the partial discharges grow and ultimately lead to complete insulation flashover.

It should be noted, additionally, that for all bridged gap data, V_i is considerably less than V_{bd} for vacuum filling but that $V_i \sim V_{bd}$ for gas. This implies that the development of the pre-breakdown processes begins at

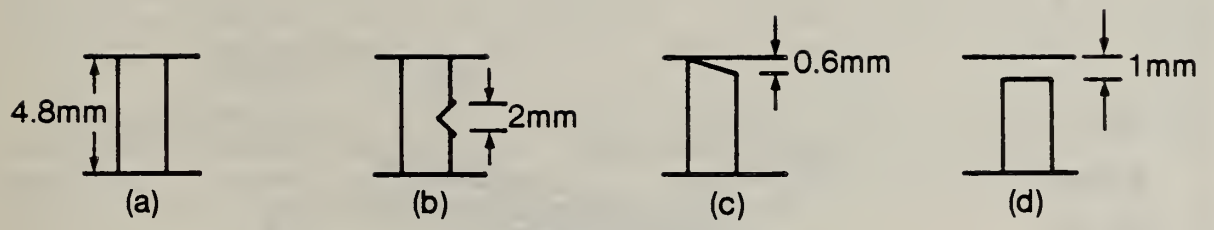

Figure 18. Insulator geometries tested.

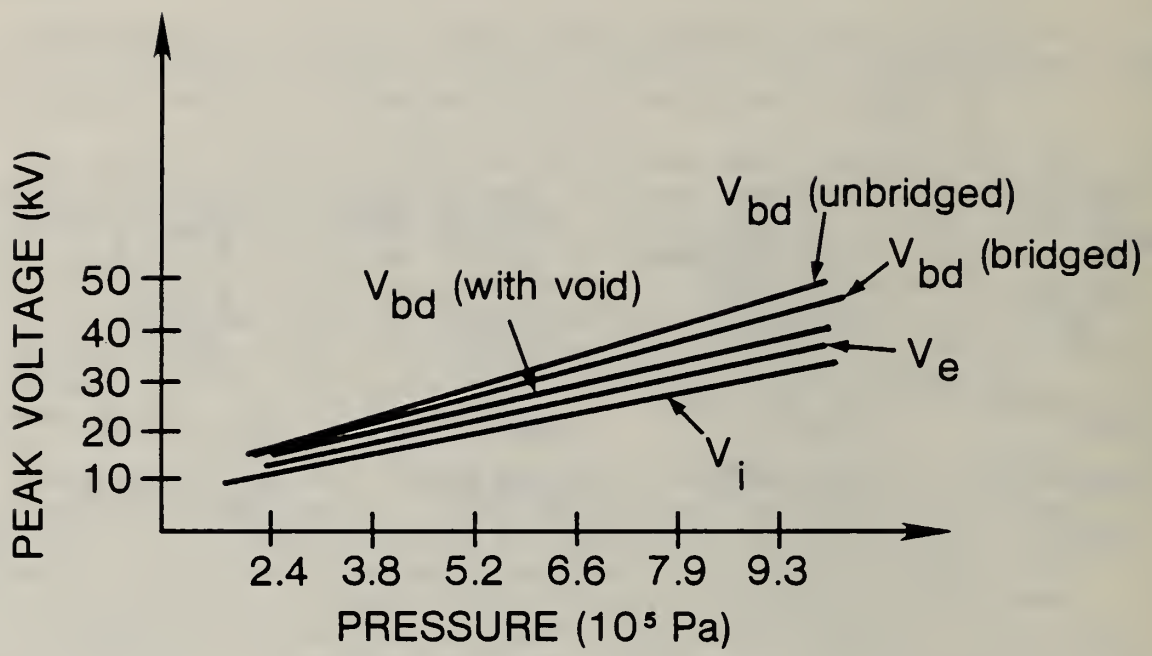

Figure 19. Breakdown, inception, and extinction voltage, 2 mm gap with void.

rather low voltages for vacuum but high voltages, essentially equal to V_{bd}, for nitrogen filled gaps.

Problems continue to be encountered in the electro-optical field measurement experiment. The system was completed this quarter. However, during final assembly the glass test vessel began to leak nitrobenzene around the window. Analysis has shown that the adhesive used to attach the window had not been properly cured. The test vessel is now being repaired, reassembled, and will soon be reinstalled. It is anticipated that electro-optical measurements of the insulator surface fields in nitrogen will be produced early during the next quarter.

A copy of the electric field analysis computer program (PLTMG), developed by Randolf Bank (now at the University of California at San Diego), has been obtained from NBS. The program has been entered into the University of South Carolina computer system, debugged, and interfaced with the University of South Carolina output graphics. Various example electrode, insulator geometries have been solved using the program. The program is now working well and is capable of solving geometries with one dielectric. Solution of this type of problem is relevant to insulator surface flashover, where a dielectric interface exists.

The electrolytic tank has been previously constructed and used. PMMA models are being machined for use in the tank. The electric fields, for the experimental geometries being used, will be determined using this analog technique and compared with the computer solutions.

Tasks to be completed next quarter include:

1. Electro-optical measurement of insulator surface fields for nitrogen and SF_6 gas.

2. Surface current and breakdown voltage measurements for nitrogen and SF_6 gas interfaces. Specifically, V_{bd} and V_i will be determined using 60 Hz ac for various insulator materials, insulator shapes, and triple junction constructions for both gases.

3. The field distributions for the geometries used in 1 and 2 above will be calculated using the computer program acquired from NBS and the electrolytic tank.

For further information, contact Dr. T. S. Sudarshan, (803) 777-7302, University of South Carolina, Columbia, SC.

7. REFERENCES

1. R. J. Van Brunt and D. A. Leep, Corona Induced Decomposition of SF_6, Gaseous Dielectrics III, Proc. of the 3rd Int'l. Symp. on Gaseous Dielectrics, Ed. by L. G. Christophorou, Pergamon Press, New York, 1982, pp. 402-409.

2. R. J. Van Brunt and M. Misakian, Role of Photodetachment in Initiation of Electric Discharges in SF_6 and O_2, J. Appl. Phys., Vol. 54, pp. 3074-3079, 1983.

3. J. W. Gallagher, E. C. Beaty, J. Dutton, and L. C. Pitchford, An Annotated Compilation and Appraisal of Electron Swarm Data in Electronegative Gases, J. Phys. Chem. Ref. Data, Vol. 12, pp. 109-152, 1983.

4. S. Hasegawa, L. Greenspan, J. W. White, and A. Wexler, A Laboratory Study of Some Performance Characteristics of an Aluminum Oxide Humidity Sensor, Nat. Bur. Stand. (U.S.) Tech. Note 824 (1974).

5. R. J. Van Brunt and D. Leep, Characterization of Point-Plane Corona Pulses in SF_6, J. Appl. Phys. Vol. 52, pp. 6588-6600, 1981.

6. M. Goldman and A. Goldman, Corona Discharges, Gaseous Electronics - Electrical Discharges, Vol. 1, Ed. by M. N. Hirsh and H. J. Oskam, Academic Press, pp. 219-290, 1978.

7. W. Becher and J. Massonne, Contribution to the Decomposition of Sulfur Hexafluoride in Electric Arcs, Elektrotech. Z., Vol. A91, pp. 605-610, 1970.

8. C. Boudene, J. L. Cluet, G. Keib, and G. Wind, Identification and Study of Some Properties of Compounds Resulting from the Decomposition of SF_6 Under the Effect of Electrical Arcing in Circuit Breakers, Revue Generale De L'Electricite (RGE) Numero Special, pp. 45-78, 1974.

9. B. Siegel and P. Breisacher, Oxidation of Sulfur Hexafluoride, J. Inorg. Nuclear Chem., Vol. 31, pp. 675-683, 1969.

10. J. Dutton, A Survey of Electron Swarm Data, J. Phys. Chem. Ref. Data, Vol. 4, pp. 577-856, 1975.

NBS-114A (REV. 2-8C)

U.S. DEPT. OF COMM. BIBLIOGRAPHIC DATA SHEET (See instructions)	1. PUBLICATION OR REPORT NO. NBSIR 84-2809	2. Performing Organ. Report No.	3. Publication Date February 1984

4. TITLE AND SUBTITLE

DEVELOPMENT OF POWER SYSTEM MEASUREMENTS -- QUARTERLY REPORT
APRIL 1, 1983 to JUNE 30, 1983

5. AUTHOR(S)

R. E. Hebner, Editor

6. PERFORMING ORGANIZATION (If joint or other than NBS, see instructions)

NATIONAL BUREAU OF STANDARDS
DEPARTMENT OF COMMERCE
WASHINGTON, D.C. 20234

7. Contract/Grant No.

8. Type of Report & Period Covered

9. SPONSORING ORGANIZATION NAME AND COMPLETE ADDRESS (Street, City, State, ZIP)

Department of Energy
Division of Electric Energy Systems
1000 Independence Avenue, SW
Washington, DC 20585

10. SUPPLEMENTARY NOTES

☐ Document describes a computer program; SF-185, FIPS Software Summary, is attached.

11. ABSTRACT (A 200-word or less factual summary of most significant information. If document includes a significant bibliography or literature survey, mention it here)

This report documents the progress on five technical investigations sponsored by the Department of Energy. Three were performed by the Electrosystems Division, the National Bureau of Standards, the fourth by the Department of Electrical Engineering of the University of Southern California, and the fifth by the College of Engineering at the University of South Carolina. The work described covers the period from April 1, 1983 to June 30, 1983. The report emphasizes the calibration of instruments designed to measure the 60-Hz electric field in biological exposure facilities, the effect of water on SF_6 corona discharges, the measurement of failure mechanisms in liquid/solid and gas/solid insulating systems, and the development and behavior of active insulators.

12. KEY WORDS (Six to twelve entries; alphabetical order; capitalize only proper names; and separate key words by semicolons)

composite insulation; electric fields; high voltage; insulation; liquid breakdown; SF_6; space charge; transformer oil

13. AVAILABILITY

☒ Unlimited

☐ For Official Distribution. Do Not Release to NTIS

☐ Order From Superintendent of Documents, U.S. Government Printing Office, Washington, D.C. 20402.

☒ Order From National Technical Information Service (NTIS), Springfield, VA. 22161

14. NO. OF PRINTED PAGES

41

15. Price

$8.50